NJC

PAPER

View Article Online
View Journal | View Issue

Cite this: *New J. Chem.*, 2014, **38**, 5349

Co(II), Ni(II) and Cu(II) complexes with phenylthiazole and thiosemicarbazone-derived ligands: synthesis, structure and cytotoxic effects†

Marta Sobiesiak,*[a] Tadeusz Muzioł,[b] Marek Rozalski,[c] Urszula Krajewska[c] and Elzbieta Budzisz[d]

Received (in Victoria, Australia) 12th June 2014,
Accepted 22nd August 2014

DOI: 10.1039/c4nj00977k

www.rsc.org/njc

Complexes of Co(II), Ni(II) and Cu(II) with 2-(3,5-dimethyl-1*H*-pyrazole-1-yl)-4-phenyl-1,3-thiazole (**a**) and 3,5-dimethyl-1*H*-pyrazole-1-carbothioamide (**b**) ligands were synthesized. The crystal and molecular structures of four of them were determined by the X-ray diffraction method. In the complexes with ligand **a** the metal atom was bound *via* two nitrogen atoms, whereas ligand **b** interacted through the nitrogen and sulfur atoms. Comparing the coordination modes observed for both studied ligands, the thiocarbamoyl sulfur atom can participate in metal binding and in bridge formation, whereas the thiazole (aromatic) sulfur atom is not involved in the coordination. This effect seems to enhance (at least partially) conformational flexibility. Hydrogen bonds played a principal role in the crystal network formation of the analyzed compounds. The cytotoxic activity of the complexes against HL-60 and NALM-6 leukemia cells and the WM-115 melanoma cell line was also measured. The copper(II) complex with the thiosemicarbazone ligand (**7b**) exhibited relatively high cytotoxicity towards all tested tumor cells. The cytotoxicity of copper(II) complexes **7b** and **9b** against the melanoma WM-115 cells was over three times higher than that of cisplatin.

Introduction

Transition metal complexes with *N*,*N*- and *N*,*S*-donor ligands have attracted remarkable attention because of their interesting chemical and biological properties. Some of these compounds induce apoptosis by activation of DNA fragmentation in cancerous cell lines.[1] Other complexes change the structure of DNA or destroy the cytoskeleton.[2] It is well known that *N* and *S* atoms play important roles in the coordination of metal ions at active sites of numerous metallobiomolecules.[3] The pharmacological properties of metal complexes depend on the properties of either the metal or the ligand. In many cases, addition of metal ions to an organic ligand can lead to the increase of its biological activity.

Thiosemicarbazone ligands are especially interesting because of their mixed hard–soft donor character, diverse coordination modes and various applications,[4] including antiviral,[5] anticancer,[6–8] antitumor,[9–11] antibacterial,[12–14] anti-inflammatory and antiamoebic[15–17] activities. Thiazole-containing chelating agents and their metal derivatives have also attracted notable interest over the years because of their various biological activities[18–20] including anticancer potency.[21–23]

Among the metal complexes, many copper(II) complexes with *N*,*N*- and *N*,*S*-donors ligands have been proposed as promising cytotoxic agents on the basis of *in vitro* assays.[24] Some of these complexes with bidentate κ^2*N*,*S*-thiosemicarbazone ligands exhibited high antiproliferative activity (at 1 to 10 μM concentration) in the HeLa (human cervical carcinoma) cancer cell line. Pyrazole–pyridine ligands and substituted bis(pyrazolyl)alkanes with *N*,*N* copper-coordinating abilities formed Cu(II) complexes with high cytotoxicity against HT1080 (human fibrosarcoma) cells.[24]

In our previous paper we described the synthesis of thiosemicarbazone derivatives and their complexes with copper(II) ions. The copper(II) complex with 3,5-dimethyl-1*H*-pyrazole-1-carbothioamide showed a 10-fold higher cytotoxicity towards the melanoma A375 cell line than the reference cisplatin. This complex was able to modify the structure of plasmid DNA by nicking the DNA form I into forms II and III and this feature may be a predominant factor for the biological activity.[25]

---

[a] *Collegium Medicum in Bydgoszcz, Nicolaus Copernicus University in Torun, Faculty of Pharmacy, Department of Inorganic and Analytical Chemistry, dr. A. Jurasza 2, 85-094 Bydgoszcz, Poland. E-mail: marta.sobiesiak@cm.umk.pl; Fax: +48 (52) 585 38 04; Tel: +48 (52) 585 38 03*

[b] *Nicolaus Copernicus University, Faculty of Chemistry, Gagarina 7, 87-100 Torun, Poland*

[c] *Department of Pharmaceutical Biochemistry, Faculty of Pharmacy, Medical University of Lodz, Muszynski 1 Str., 90-151 Lodz, Poland*

[d] *Department of Cosmetic Raw Materials Chemistry, Faculty of Pharmacy, Medical University of Lodz, Muszynski 1 Str., 90-151 Lodz, Poland*

† Electronic supplementary information (ESI) available. CCDC 988739 (**1a**), 988743 (**6a**), 989127 (**8a**) and 988741 (**5b**). For ESI and crystallographic data in CIF or other electronic format see DOI: 10.1039/c4nj00977k

The ability of 3,5-dimethyl-1*H*-pyrazole-1-carbothioamide to complex several transition metal ions has been previously tested. It has been reported that the molecular structure of the resulting complexes depends primarily on the characteristic bonding preferences of the central metal ion and on the nature of the anion.[26,27] However, there is no report on the synthesis of metal complexes with 4-phenylthiazole derivatives generated from 2-(3,5-dimethyl-1*H*-pyrazole-1-yl)-4-phenyl-1,3-thiazole.

We examined two types of *N*,*N*- and *N*,*S*-donor chelators and here we present the synthesis and structural characterization of some new cobalt(II), nickel(II) and copper(II) complexes with 2-(3,5-dimethyl-1*H*-pyrazole-1-yl)-4-phenyl-1,3-thiazole (ligand **a**), and with 3,5-dimethyl-1*H*-pyrazole-1-carbothioamide (ligand **b**). The resulting complexes were evaluated for their cytotoxic activity against three tumor cell lines.

Results and discussion

Chemistry

The 4-phenylthiazole ligand (**a**) and the thiosemicarbazone ligand (**b**) (Fig. 1) were synthesized according to the procedure described in the Experimental section. The general method employed to prepare the final compounds is outlined in Scheme 1. Both ligands in the reactions with metal(II) salts yielded complexes **1a–9a** and **1b–9b** as solids.

In the complexes with ligand **a**, the metals ions were coordinated by the two nitrogen atoms of the ligand, while the sulfur atom did not take part in the coordination. The 4-phenylthiazole compound reacted in ethyl acetate–methanol solutions with metal(II) chloride hexahydrate or metal(II) nitrate hexahydrate in a 1 : 1 molar ratio to yield [$MLCl_2$] complexes **1a** and **7a** or [$ML(NO_3)_2$] complexes **2a** and **5a**. Surprisingly, copper(II) nitrate trihydrate and this ligand formed an ionic complex **8a** with general structure $[CuL_2NO_3]_2^{+}[Cu(NO_3)_4]^{2-}$. Ligand **a** with metal(II) perchlorate hexahydrate in ethyl acetate solution formed complexes **3a**, **6a**, and **9a**, in a molar ratio of 2 : 1.

The course of complex formation by thiosemicarbazone is anion-dependent and may be explained on the basis of Pearson's theory, taking into account the steric factors.[28] The thiosemicarbazone derivative (**b**) has three potential coordination sites: the nitrogen atom of the pyrazole ring and the nitrogen and sulfur atoms of the thiocarbamoyl group. That ligand may act as a neutral bi- or monodentate moiety.[26] In our experiments, ligand **b** interacted with the metal ions (in metal(II) chlorides, metal(II) nitrates or metal(II) perchlorates) as a bidentate *N*,*S*-donor to form the corresponding five-membered chelate rings. In the Co(II) and Cu(II) complexes, obtained by a reaction of $CoCl_2·6H_2O$ and $CuCl_2·3H_2O$ with the pyrazole derivative (**b**), the ligand coordinates to the metal in the same way as in the compounds described by Radosavljević Evans *et al.*[26] In the ethyl acetate–methanol solution of $CoCl_2$ and $CuCl_2$, the large, moderately "soft" Co(II) and Cu(II) cations preferentially bond to the "soft" *S* atom, resulting in *N*,*S* coordination. Mészáros Szécsényi *et al.*[27] reported the structures of ligand **b** with nickel(II) salts in which Ni(II) preferentially binds to the "hard" base *N* atom of the thioamide group (carrying a deprotonated NH_2 function), resulting in *N*,*N* coordination of the ligand. In this work we obtained nickel(II) compounds wherein chelation of 3,5-dimethyl-1-thiocarboxamide pyrazole occurs through a "soft" base *S* atom of the thioamide group. Ligand (**b**) reacted in ethyl acetate–methanol solutions with metal(II) chloride hexahydrate or metal(II) nitrate hexahydrate in a 1 : 1 molar ratio to yield [$MLCl_2$] complexes **1b**, **4b**, and **7b** or [$ML(NO_3)_2$] complex **8b**. Nickel(II) nitrate hexahydrate and ligand **b** formed complex **5b** in a molar ratio of 2 : 1, irrespective of the L : M substrate molar ratio (1 : 1 or 2 : 1). The reaction of ligand **b** with cobalt(II) perchlorate hexahydrate in ethyl acetate solution formed complex **3b** in a molar ratio of 2 : 1. However, complexes **6b** and **9b** (ligand **b** and nickel(II) or copper(II) perchlorate hexahydrate) were formed in a molar ratio of 3 : 1, irrespective of the L : M substrate molar ratio (2 : 1 or 3 : 1). The molecular structure of a representative complex $[NiL_2(NO_3)](NO_3)$ (Fig. 5) was determined by X-ray crystallography.

Neither cobalt(II) nitrate and ligand **a** nor nickel(II) chloride and ligand **b** created the expected complexes.

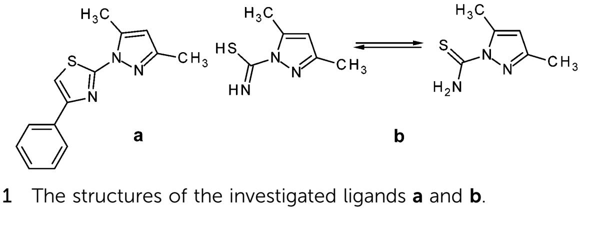

Fig. 1 The structures of the investigated ligands **a** and **b**.

Characterization of ligands and metal complexes

Comparative analysis of the infrared spectra of the complexes and the metal-free ligands has revealed that the absorption bands characteristic of the stretching vibrations of the pyrazole ν(C=N) group shifted from 1603 cm^{-1} and 1600 cm^{-1} for ligands **a** and **b** to higher frequencies at 1626–1647 cm^{-1} for their complexes. This observation can be explained by the participation of the nitrogen atom of pyrazole in the coordination with metal ions in complexes. The band in the 1502–1511 cm^{-1} region of complexes with ligand **a** has been assigned to ν(C=N) of the thiazole moiety. For these complexes, this characteristic band shifted by 23–32 cm^{-1} to higher frequency in comparison with the spectrum of the ligand (*ca.* 1479 cm^{-1}). The infrared spectra of ligand **a** and its complexes (**1a–9a**) showed no changes in the absorption bands attributed to the vibrations of the ν(C=S) group in the 685–700 cm^{-1} region. These data indicate that ligand–metal bonds in these complexes involved the nitrogen atoms and not the sulfur atoms of the thiazole ring.

The characteristic bands at 3083–3107 cm^{-1} and 2976–2995 cm^{-1} of the methyl group of ligands **a** and **b** and their complexes were assigned to ν(C–H) vibration, respectively.

The FTIR spectra of ligand **b** and its complexes exhibited strong bands at 3400–3100 cm^{-1} due to $\nu(NH_2)$ vibration of the primary amide group. The NH_2 bands in the spectrum of the ligand appeared at 3388 cm^{-1} (NH_2 stretch), 3241 cm^{-1} (asymmetric stretch) and 3134 cm^{-1} (symmetric stretch).[27] An intense strong band at 880 cm^{-1} and a moderate one at

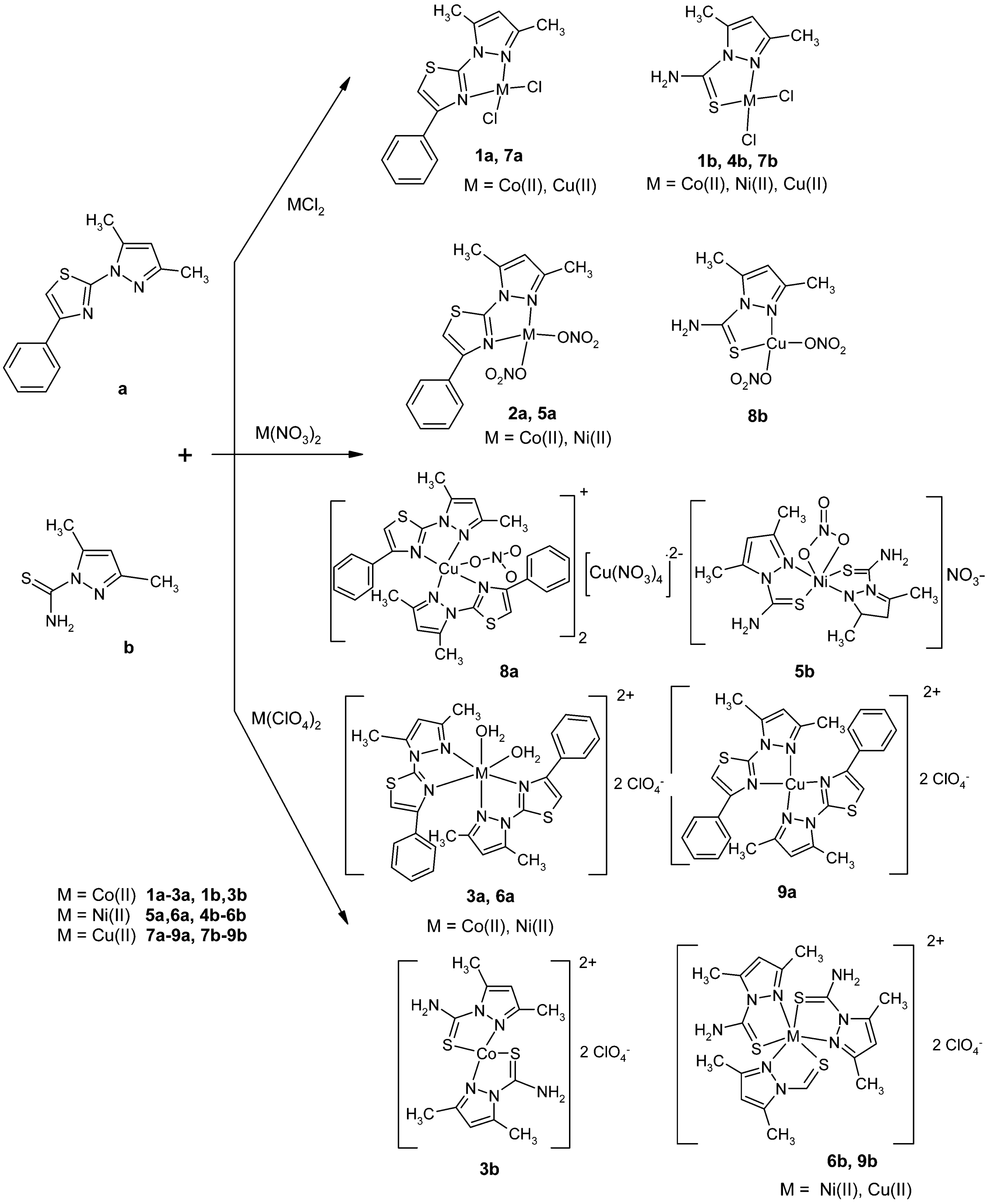

Scheme 1 Synthesis and proposed structures of the Co(II), Ni(II), Cu(II) complexes **1a–9a**, **1b–9b** with ligands **a** and **b**.

808 cm^{-1} in the spectrum of this ligand (the ν(C=S) vibration) shifted to lower frequencies (863–812 cm^{-1} and 783–750 cm^{-1}, respectively) in the spectra of **1b–9b** complexes, suggesting the sulfur atom of $>$C=S to be a possible site of metal coordination.

Complexes **3a**, **6a**, **9a**, **3b**, **6b**, and **9b** showed intense bands at 1120–1085 cm^{-1} due to the involvement of the perchlorate ion, and a sharp band of medium intensity at 629–623 cm^{-1} characteristic of uncoordinated perchlorate ions. The presence of two bands between 1379–1383 cm^{-1} (very strong) and at 810–845 cm^{-1} (medium) showed that complexes **2a**, **5a**, **8a**, **5b** and **8b** include the NO_3^- ions in their structure.[9]

The chemical shifts and intensities of the signals in the ^{1}H NMR spectra of ligands **a** and **b** were very much similar to those in the spectra recorded for the corresponding nickel(II) complexes **5a**, **6a**, and **4b–6b**. The spectra were recorded in DMSO-d$_6$ and are presented in the Experimental section.

The ligands and complexes showed signals in the range of δ 2.15–2.80 ppm for the methyl groups and δ 5.92–6.29 ppm for the proton of the pyrazole ring. In the spectrum of ligand **a** and its complexes we observed a signal at $\delta \sim 7.80$ ppm for the proton from the thiazole moiety and at δ 7.30–7.90 ppm for the protons from the phenyl group. The amine protons from ligand **b** were seen as two singlets at δ 9.13 and 9.54 ppm for ligand **5a** and at δ 8.86–9.10 ppm and δ 9.27–9.51 ppm for complexes **4b–6b**. The presence of two singlets for the two NH_2 protons may indicate some involvement in hydrogen bonding. Although these protons are not directly involved in metal coordination, their signals tend to be shielded, perhaps due to inductive effects.[7]

The ^1H NMR spectra of cobalt(II) and copper(II) complexes could not be measured due to their paramagnetism.

The metal complexes have been investigated by mass spectrometry. The parent ions of complexes have not been observed in the mass spectra. However, in the FAB-MS spectra of all complex compounds the ions attributable to $[LM]^+$ (L = **a**, **b**, M = Co(II), Ni(II), Cu(II)) were observed. The molecular ions corresponding to compounds $[L_2M]^+$ have been found for complexes **3a**, **6a**, **9a**, **3b**, **5b**, and **6b**. Additionally, $[LMCl]^+$ ions for **1a**, **7a**, **1b**, **4b**, and **7b**, as well as $[LMNO_3]^+$ ions for **2a**, **5a**, **5b**, and **8b** and $[LMClO_4]^+$ ions for **3a**, **6a**, **9a**, and **3b** were found. Furthermore, $[L_2MNO_3]^+$ and $[L_2MClO_4]^+$ ions were observed in the FAB-MS spectra of coordination complexes **2a**, **5a**, **8a**, **5b**, **8b** and **6a**, **3b**, **6b**, **9b**, respectively. The FAB-MS spectra of complexes **1b–9b** presented ion peaks at (m/z) 256, corresponding to L + 1H. Additionally, mass spectrometry showed the presence of $[CuL_2NO_3]_2[Cu(NO_3)_4]$ ions **8a**. This is evidenced by the fact that FAB produced $[CuL]^+$ $[CuL_2]^{2+}$ and $[CuL_2NO_3]^+$ ions (observed in positive ion mode) and the $[Cu(NO_3)_4]^{2-}$ and $[Cu(NO_3)_2]^-$ ions (observed in negative ion mode). The most structurally informative fragment ions in the positive-ion mode of complexes **1a–9a**, **1b–9b** are presented in Table S1 (ESI†).

Molecular structures of 1a, 6a, 8a and 5b

Herein we report the structures of $[Co(\mathbf{a})Cl_2]$ (**1a**), *cis*-$[Ni(\mathbf{a})_2(H_2O)_2](ClO_4)_2$ (**6a**), $[Cu(\mathbf{a})_2(NO_3)]_2[Cu(NO_3)_4]$ (**8a**) and $[Ni(\mathbf{b})_2NO_3](NO_3)\cdot 0.9OEt_2\cdot 0.4H_2O$ (**5b**). The details of the refinement of all compounds reported in this paper are presented in Table 1.

$[Co(\mathbf{a})Cl_2]$ (**1a**) crystallized in the monoclinic $P2_1/n$ space group with all atoms in general positions and the whole molecule given by the formulae in the asymmetric unit (Fig. 2). In (**1**) the coordination sphere around the Co atom adopts a significantly distorted tetrahedral environment. The coordination sphere consists of two nitrogen atoms and two chlorine atoms. The N1–Co1–N10 angle is very small [80.28(7)°], whereas all other angles exceed 110° (Table S2, ESI†). Co1–N1 is the shortest [2.0087(19) Å] in the coordination sphere and Co1–N10 is longer [2.0782(18) Å] by 0.07 Å. Both chlorine atoms are bound to the Co atom at the same distance within experimental error [2.2064(6) and 2.2090(6) Å]. All rings are flat with maximal deviation for the chelate ring reaching 0.01 Å and are coplanar with the biggest angle 1.24° between the pyrazole and the chelate rings. It is interesting that also the phenyl ring remains

Table 1 Crystal data and structure refinement for (**1a**), (**6a**), (**8a**) and (**5b**)

Parameters	1a	6a	8a	5b
Empirical formula	$C_{14}H_{13}Cl_2CoN_3S$	$C_{28}H_{30}Cl_2N_6NiO_{10}S_2$	$C_{56}H_{52}Cu_3N_{18}O_{18}S_4$	$C_{15.6}H_{27.8}N_8NiO_{7.3}S_2$
Formula weight	385.16	804.31	1584.02	567.09
Temperature [K]	293(2)	293(2)	293(2)	293(2)
Wavelength [Å]	0.71073	0.71073	0.71073	0.71073
Crystal system, space group	Monoclinic, $P2(1)/n$	Monoclinic, $C2/c$	Orthorhombic, $Pbcn$	Monoclinic, $P2(1)/n$
Unit cell dimensions [Å] and [°]	a = 8.9069(4)	a = 24.0372(10)	a = 19.8159(6)	a = 16.6552(6)
	b = 14.7753(6)	b = 9.6174(3)	b = 13.1908(6)	b = 14.1497(5)
	c = 12.3744(5)	c = 16.0976(7)	c = 25.0863(9)	c = 23.1221(10)
	β = 102.793(4)	β = 113.255(5)		β = 104.258(4)
Volume [Å^3]	1588.07(12)	3419.0(2)	6557.2(4)	5281.2(4)
Z, calculated density [mg m^{-3}]	4, 1.611	4, 1.563	4, 1.605	8, 1.426
Absorption coefficient [mm^{-1}]	1.543	0.909	1.176	0.943
F(000)	780	1656	3236	2366
Crystal size [mm]	0.55 × 0.28 × 0.18	0.98 × 0.58 × 0.27	0.26 × 0.17 × 0.15	0.34 × 0.26 × 0.13
Theta range for data collection [°]	2.18 to 26.37	2.31 to 26.37	2.02 to 26.37	2.32 to 25.03
Limiting indices	$-11 \le h \le 11$	$-30 \le h \le 14$	$-7 \le h \le 24$	$-16 \le h \le 19$
	$-18 \le k \le 15$	$-10 \le k \le 12$	$-10 \le k \le 16$	$-7 \le k \le 16$
	$-6 \le l \le 15$	$-17 \le l \le 20$	$-20 \le l \le 31$	$-27 \le l \le 19$
Reflections collected/unique	5674/3246 [R(int) = 0.0362]	5751/3494 [R(int) = 0.0849]	16 524/6694 [R(int) = 0.0534]	17 920/9384 [R(int) = 0.0792]
Completeness to theta	26.37° 99.9%	26.37° 99.8%	26.37° 99.7%	25.03° 99.9%
Absorption correction	Numerical	Numerical	Numerical	Numerical
Max. and min. transmission	0.7686 and 0.4841	0.7913 and 0.4694	0.8433 and 0.7496	0.8872 and 0.7399
Refinement method	Full-matrix least-squares on F^2	Full-matrix least-squares on F^2	Full-matrix least-squares on F^2	Full-matrix least-squares on F^2
Data/restraints/parameters	3246/0/192	3494/0/231	6694/0/450	9384/6/635
Goodness-of-fit on F^2	0.873	1.068	0.942	1.042
Final R indices [$I > 2\sigma(I)$]	$R_1{}^a$ = 0.0320, w$R_2{}^b$ = 0.0920	$R_1{}^a$ = 0.0458, w$R_2{}^b$ = 0.1279	$R_1{}^a$ = 0.0459, w$R_2{}^b$ = 0.1021	$R_1{}^a$ = 0.0720, w$R_2{}^b$ = 0.2057
R indices (all data)	$R_1{}^a$ = 0.0403, w$R_2{}^b$ = 0.0963	$R_1{}^a$ = 0.0528, w$R_2{}^b$ = 0.1320	$R_1{}^a$ = 0.1010, w$R_2{}^b$ = 0.1230	$R_1{}^a$ = 0.1445, w$R_2{}^b$ = 0.2381
Extinction coefficient	—	0.0008(4)	—	—
Largest diff. peak and hole [e Å^{-3}]	0.327 and −0.312	0.706 and −0.440	0.810 and −0.893	0.460 and −0.430

[a] $R_1 = \sum||F_0| - |F_c||/\sum|F_0|$. [b] $wR_2 = [\sum w(F_0{}^2 - F_c{}^2)^2/\sum(w(F_0{}^2)^2)]^{1/2}$.

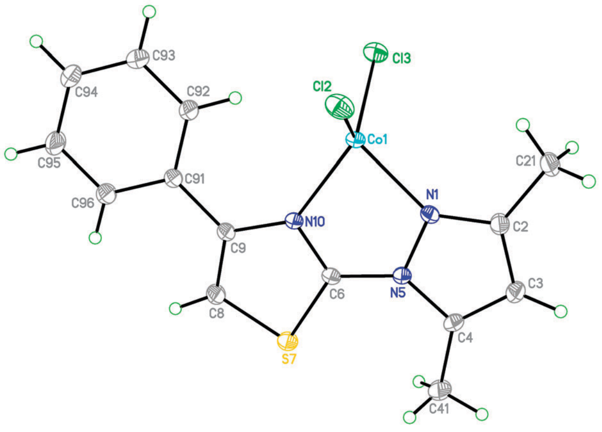

Fig. 2 Molecular structure of complex **1a** with the numbering scheme and the displacement ellipsoids drawn at the 20% probability level.

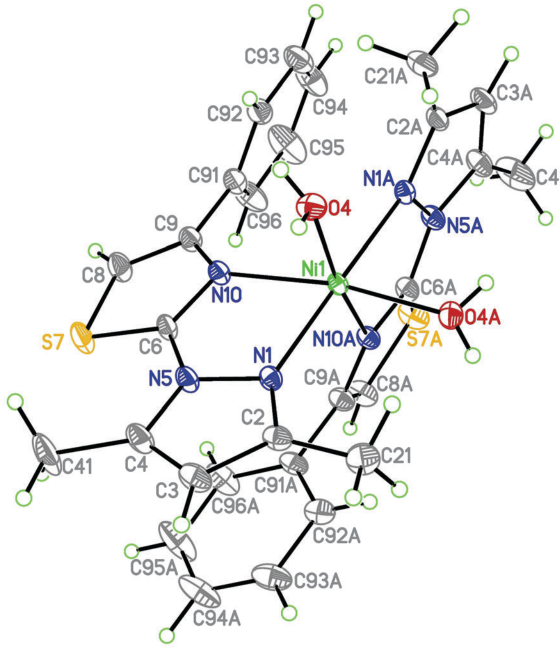

Fig. 3 Molecule of *cis*-$[Ni(\mathbf{a})_2(H_2O)_2](ClO_4)_2$ (**6a**) with the numbering scheme and the thermal ellipsoids at 20% probability. For the clarity of the figure the perchlorate ion is omitted.

coplanar with these three rings and it forms angles not exceeding 9.12°. It happens often that such phenyl rings are significantly twisted. In this case the conformation of the organic ligand results from the packing revealing all aromatic rings in the *ac* layer and the intramolecular hydrogen bond is formed between H92 and N10 atoms. Hence, the separation between the layers is maintained by chloride ions. As a consequence, the Co–Co distance is much bigger inside one layer (at least 8.907 Å) than between layers (the shortest distance between the layers is 7.504 Å). Therefore, the molecules inside one layer interact weakly creating only two hydrogen bonds: H41C–Cl3$(1 + x, y, z)$ and H41B–Cl2$(1 + x, y, z)$. In the crystal network of (**1a**) the π–π interactions dominate between the systems being fairly coplanar (Fig. S1, ESI†).

cis-$[Ni(\mathbf{b})_2(H_2O)_2](ClO_4)_2$ (**6a**) crystallized in the monoclinic *C*2/*c* space group with the nickel ion positioned at the twofold axis. In the asymmetric unit there are the nickel ion, the organic ligand, one coordinated water molecule and a perchlorate anion (Fig. 3). The nickel ion is found in an octahedral environment with four nitrogen atoms from organic ligands (both N1 nitrogen atoms are found in *trans* positions) and two oxygen atoms from water molecules found in *cis* positions. In the nickel coordination sphere, Ni–N bonds are 2.091(2) Å for Ni1–N1 and 2.1417(18) Å for Ni1–N10, whereas Ni–O bonds are much shorter being 2.0692(17) Å long (Table S2, ESI†). The valence angles deviate from 78.25(7) to 104.39(7)° and from 170.11(7) to 176.51(9)° with the smallest angles close to 80° found for the five-membered chelate rings.

All aromatic rings remain flat with rms deviation reaching 0.003 Å, whereas the chelate ring is slightly folded with rms of 0.032 Å. The angle between S7 and N1 rings of the ligand molecule reaches 14.52° showing that the fused ring system in this molecule is quite folded. The C91 phenyl ring is significantly inclined up to 69.67° to other rings. This conformation of the ligand enables numerous strong (due to mutual orientation) π–π interactions between two ligands coordinated to the same nickel(II) ion. Apart from that C21–H21C···O4$(-x + 1, y, -z + 1/2)$ and an intramolecular C41–H41B···S7 hydrogen bond are formed.

In the packing (Fig. S2, ESI†) we observe well-ordered structure in all three dimensions with significant separation of at least 9.341 Å between nickel(II). Due to the distances between the metal ions we describe this packing as *bc* layers with the angle of only 61.70° between three closest nickel(II) ions. Hence, the nickel ions in the layer are arranged in almost perfect rhombuses with the sides being 9.341$(1 - x, -y, 1 - z)$ Å and 9.617$(x, 1 + y, z)$ Å long and the shorter diagonal of 9.412$(1 - x, 1 - y, 1 - z)$ Å, whereas the distance between the adjacent layers exceeds 11 Å. In the crystal network formation numerous π–π interactions play the main role, among them a system of stacking interactions composed of four rings: C91(x, y, z)–S7(x, y, z)–S7$(1 - x, 1 - y, 1 - z)$–C91$(1 - x, 1 - y, 1 - z)$. Hence, the intermolecular interactions between two S7 rings are capped by two C91 phenyl rings inclined only by 4.36° and forming intramolecular stacking interaction. Additionally, the closest molecules interact *via* a hydrogen bond network created by both coordinated O4 water molecules and four perchlorate ions revealing the importance of these ions. They fasten the network participating in hydrogen bonds as well as Cl–O···π interactions.

$[Cu(\mathbf{a})_2(NO_3)]_2[Cu(NO_3)_4]$ (**8a**) crystallized in the orthorhombic *Pbcn* space group with a Cu2 atom positioned at the *b* twofold axis. Hence, in the asymmetric unit there is one $[Cu(\mathbf{a})_2(NO_3)]^+$ moiety and the Cu2 atom with two nitrate anions (Fig. 4a and b). Cu1 atoms exist in a square pyramidal environment with the trigonal distortion parameter $\tau = 0.20$[29] and the coordination sphere is composed of four nitrogen atoms from two organic ligands as well as one oxygen atom from the nitrate ion. The Cu–N bonds range from 1.982(3) to 2.275(3) Å (Table S2, ESI†). The longest value occurring for the apical atom reveals elongation due to the Jahn–Teller effect. The length of 1.988(3) Å for the

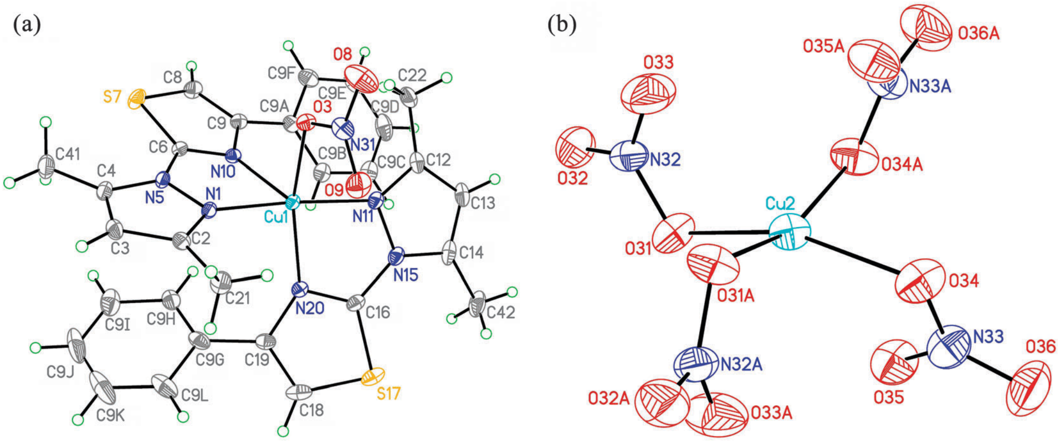

Fig. 4 Molecule of $[Cu(\mathbf{a})_2(NO_3)]_2[Cu(NO_3)_4]$ (**8a**) with the numbering scheme and the thermal ellipsoids at 20% probability. In the asymmetric unit there is one $[Cu(\mathbf{a})_2(NO_3)]^+$ cation (a) and Cu2 copper cation with two nitrate anions from the $[Cu(NO_3)_4]^{2-}$ unit (b).

Cu1–O3 bond is similar to the values observed for Cu1–N1 and Cu1–N11 bonds, whereas the forth basal Cu–N bond is elongated by 0.06 Å [Cu–N20: 2.045(3) Å]. In the coordination sphere valence angles fall in two ranges: from 77.50(11) to 108.42(12)° and from 161.67(12) to 173.98(12)°. In the second moiety the Cu2 ion is surrounded by four nitrate anions monodentately coordinated, which form a significantly distorted tetrahedral environment with Cu–N distances of 1.975(4) and 1.984(4) Å and the angles falling into two ranges: close to 90° and 158°.

All aromatic rings remain flat with rms deviation reaching 0.014 Å for the S17 ring. The chelate rings are much more folded with rms 0.084 and 0.057 Å for N11 and N1 rings, respectively. All fused rings in one ligand are rather flat with the biggest angles of 17.7 and 14.0° created for S17 and S7 ligands, respectively. In complex **8a** both phenyl rings are significantly twisted like the fused rings with an angle close to 50° and 40° for S17 and S7 ligands, respectively. The angle formed between S7 and S17 molecules is 52.20° indicating that the orientation of both ligands is significantly tilted. Several intramolecular π–π interactions determine such mutual orientation of these rings. Additionally, C–H···π interactions and hydrogen bonds between the methyl groups and O3 or sulfur atoms were detected.

The packing viewed along the *a* axis reveals *ab* layers of $[Cu(L')_2(NO_3)]^+$ cations, which are separated by layers of $[Cu(NO_3)_4]^{2-}$ anions (Fig. 5). In the network we observe strong interactions, which are assured mainly by hydrogen bonds and π–π interactions. Despite the separation of cation layers by $[Cu(NO_3)_4]^{2-}$ anions, they form direct π–π interactions between C9A(x, y, z) and C9G(x, $1 - y$, $-1/2 + z$) phenyl rings. However, interlayer interactions are transferred mainly by $[Cu(NO_3)_4]^{2-}$ moieties involved in hydrogen bonds and N32–O32···N1(x, y, z) pyrazole ring interactions.

$[Ni(\mathbf{b})_2NO_3](NO_3)\cdot 0.9OEt_2\cdot 0.4H_2O$ (**5b**) crystallized in the monoclinic $P2_1/n$ space group with two nickel-containing moieties in the asymmetric unit (Fig. 6a and b). Additionally in the asymmetric unit there are two nitrate ions, two diethyl ether molecules (one of them occurs with 0.8 occupancy) and a water molecule (0.8 occupancy). Both nickel ions are found in an octahedral environment with two nitrogen and two sulfur atoms from organic ligands and two oxygen atoms from nitrate anions. The oxygen atoms occupy *cis* positions and are *trans* to the sulfur atoms. Hence, both nitrogen atoms forming the shortest bonds to the nickel ion are found in *trans* positions. The Ni–N bonds range from 2.033(5) Å for Ni1–N11 to 2.070(6) Å for Ni1–N1 bonds (Table S2, ESI†). The Ni–O bonds are longer and fall in a very broad range from 2.100(5) to 2.212(6) Å. The longest bonds are created by the sulfur atoms, which participate in coordination instead of the N10 atoms. They range from 2.333(3) to 2.374(2) Å. However, N10 atoms are not aromatic as in the L′ ligand and bear two hydrogen atoms (in our model we found three positions with 0.67 occupancy each). The coordination spheres reveal significant distortions as suggested by the valence angles falling into two ranges: from 59.6(2)° to 104.1(2)° and from 153.0(2)° to 178.7(2)° for the Ni1 atom and from 59.7(2)° to 105.14(9)° and from 155.2(2)° to 176.1(3)° for the Ni2 coordination sphere. 104.1(2)° and 105.14(9)° were found for S–Ni–S angles. Among *trans* positioned atoms the biggest values

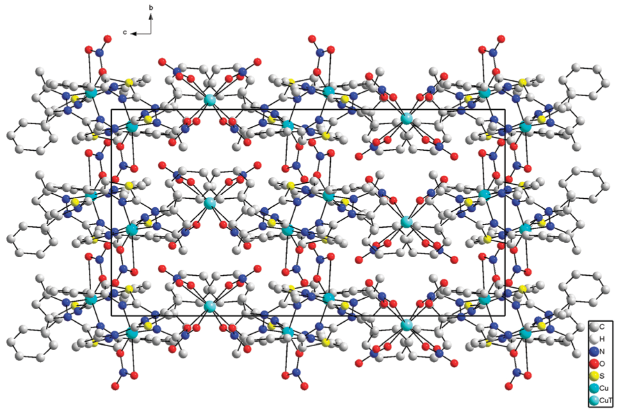

Fig. 5 Crystal network of (**8a**) along the *a* axis. For clarity of the figure all hydrogen atoms are omitted. CuT denotes tetrahedral copper(II) ions coordinated by four nitrates.

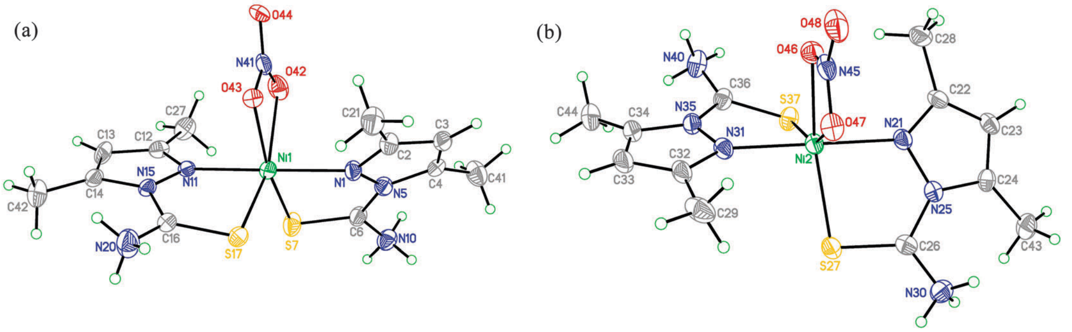

Fig. 6 Molecule of $[Ni(\mathbf{b})_2NO_3](NO_3)\cdot0.9OEt_2\cdot0.4H_2O$ (**5b**) with the thermal ellipsoids at 20% probability. Only two Ni units are presented with the numbering scheme (a, b) whereas the non-coordinated nitrates, diethyl ether and water molecules are omitted for clarity of the picture.

were found for the N–Ni–N angles, whereas the O–Ni–S angles are smaller revealing larger deviation from 180°. The smallest angle occurs for bidentately coordinated nitrate anions, which are involved in the formation of the four-membered chelate rings. The small size of this anion does not permit for the appropriate occupation of two adjacent positions in the regular octahedron and the deformation of the octahedral nickel environment is a consequence of the smaller size and the rigid structure of the nitrate anion. All aromatic rings remain flat with rms deviation reaching 0.012 Å, whereas the chelate ring is significantly folded with rms up to 0.141 Å. Pyrazole and chelate rings are not coplanar and are inclined at an angle ranging from 10.9(4)° to 13.2(4)°. This results in the shift of N10 from the chelate ring plane, which reveals a very broad range: from 0.0543 Å for N10 to −0.6830 Å for N40. The angles between the organic ligands and the coordinated nitrate anion bound to the same nickel ion are almost perpendicular with values being close to 80–90°. Two organic ligands coordinated to the same nickel ion are inclined by approximately 60°.

In the packing we observe *ab* layers with nickel ions from adjacent layers separated at least by 11.574 Å. Every layer is composed of both nickel units. In a single layer there are almost equally distributed nickel units. Every nickel unit is surrounded by six other moieties with Ni–Ni distances ranging from 7.802 to 8.783 Å. The Ni1 block is surrounded by two other Ni1 units and four Ni2 units, whereas Ni2 is surrounded by two Ni2 and four Ni1 units. Every layer is composed of alternately arranged Ni2 and Ni1 zigzags with Ni2–Ni2 and Ni1–Ni1 distances of 7.802 and 7.854 Å, respectively. These values correspond to the shortest intermetallic distances in the crystal network and they are slightly shorter for Ni2–Ni2 contacts due to a slightly bigger value of the Ni2–Ni2–Ni2 angle (130.12 *vs.* 128.51°). In the crystal packing the interactions the inside *ab* layer are transmitted directly between nickel moieties *via* numerous π–π interactions mainly created by the edge-to-face oriented pyrazole rings. Additionally, there are N–O···π interactions occurring in Ni1 and Ni2 zigzags. Moreover, this network reveals a robust network of hydrogen bonds. However, there are only a few examples of direct interactions between nickel subunits and only in one layer, whereas nickel moieties from adjacent layers do not interact directly. Such hydrogen bonds are created by C–H bonds of the pyrazole ring or its methyl substituents and the coordinated nitrate anions. Apart from that, there are numerous N–H···O interactions created between the non-coordinated amine group and also non-coordinated nitrate anions. Hence, we can hypothesize that these anions are very important for the crystal network formation, because they are involved in the interactions with nickel subunits from the adjacent layers. Similarly, an ether molecule also mediates interaction between the adjacent layers (Fig. S3, ESI†).

In this paper we report structures of complexes containing two related ligands. In all compounds reported in this paper the organic ligand coordinate *via* the N1 pyrazole nitrogen atom and in three cases also *via* the N10 thiazole nitrogen atom. We observe that the thiazole sulfur atom is not involved in the coordination while the aliphatic sulfur exerts high affinity towards nickel as evidenced in complex **5b**. For M–N1 metal–pyrazole bonds the distances range from 1.982(3) Å for the copper complex to 2.091(2) Å for the nickel complex (**6a**). In general, we observe that these distances are usually close to 2 Å, but differ quite significantly for both nickel complexes. The M–N10 distance varies from 2.045(3) to 2.275(3) Å and both extreme values were found for the copper complex. This bond is usually about 0.05–0.07 Å longer than the metal–pyrazole nitrogen bond and only for the Cu1–N10 bond in complex **8a** this elongation is much bigger reaching 0.3 Å. It is worth noticing that in the reported structures we found two kinds of nitrate coordination: monodentately in complex **8a** and bidentately in **5b**. In the latter case the small dimensions resulted in significant distortions of the coordination sphere geometry.

There are several interesting papers reporting related ligands with cobalt, copper, nickel, zinc, cadmium and palladium ions.[30,31] Due to the diversity of the known structures in terms of metal as well as ligands we decided to discuss these structures together and to compare with compounds reported in this paper. Bolos *et al.* reported the structure of a copper complex with 2-amino-5-methyl-1,3-thiazole, which is related to ligand **a** because it possesses a thiazole ring.[32] It is coordinated monodentately *via* the aromatic nitrogen atom with $Cu–N_{thiazole}$ bonds being 1.945(6) and 2.063(7) Å. The former bond is much shorter than the corresponding bond found in **8a**. Other copper complexes are known with ligands related to the **b** ligand.[26,30] In the bidentately coordinated L ligand in two complexes formulated as $[Cu_2(NCS)_4(L)_2]$ and $[Cu(NO_3)_2(L)_2]$ (L = 3,5-dimethyl-1*H*-pyrazole-1-carboxamidine) the sulfur atom is substituted by a nitrogen atom.[30] The Cu–N1 distances [1.983(3) and 2.0221(14) Å] are similar to those in our copper complex. In contrast, Cu–N3$_{pyrazole}$ distances [1.952(3) and 1.9457(15) Å] are significantly shorter than Cu–N10 bonds observed in complex **8a** with the N10 thiazole nitrogen atom involved in the coordination. In two copper complexes two molecules of the **b** ligand were bound to metal ions *via* nitrogen and sulfur atoms.[26] The copper atom was found in trigonal bipyramidal or tetrahedral environments and Cu–N distances differed being 1.984(4) Å in the pentacoordinated complex and 2.023(3) Å in the tetrahedral one. These distances are similar to Cu–N1 bond lengths in **8a**. However, Radosavljević *et al.* showed that the sulfur atom may be involved in the bridging of two copper ions and the Cu–S bond lengths depend on the binding mode. They are 2.308(1) Å in the pentacoordinated complex, whereas an elongation is observed [2.341(1) and 2.522(1) Å] if the sulfur atom is involved in bridge formation. We found coordination *via* sulfur only in the case of nickel complex **5b** with Ni–S bond lengths similar to the values observed for bridging Cu–S bonds. Radosavljević *et al.* reported the structure of 3,5-dimethyl-1-thiocarboxamidopyrazole complexed with nickel(II) in a square planar environment of four nitrogen atoms bound at an average distance of 1.902 Å.[33] In octahedral complexes **6a** and **5b** the Ni–N1 bond lengths range from 2.033(5) to 2.091(2) Å, so they are remarkably longer than those described in the literature. Moreover, there are four nitrogen atoms in the coordination sphere in **6a**, but Cu–N$_{pyrazole}$ distances are significantly shorter than the Cu–N$_{thiazole}$ bonds. In the cobalt(II) complex with two molecules of the **b** ligand the metal ion was found in a trigonal bipyramidal environment. The metal ion is coordinated *via* nitrogen and sulfur atoms of the **b** ligand with the Co–N distance of 2.108(1) Å[26] which is much longer than the Co–N1 bonds in **1a**.

We evaluated dihedral angles between the rings in all ligands present in the four reported compounds (Table S3, ESI†). Only in the cobalt(II) complex **1a** all rings are nearly coplanar and even the phenyl group remains in the plane of three other rings (very small rms for these rings). In three other structures the rings are not so perfectly coplanar. The most important deviation was found for the phenyl rings, in **6a** and **8a**, which are twisted by 52–70° towards the pyrazole ring due to numerous intramolecular π–π interactions and hydrogen bonds. In the zinc(II) structure, these rings are twisted by −5.6(2)° and 27.4(2)°.[31] This difference results from steric hindrance between both phenyl rings coming from the neighboring molecules. These authors also found that in the molecules neighboring along the *c* axis both phenyl rings are perpendicularly oriented [88.2(2)°]. In our compounds, the biggest values of dihedral angles between the C91 phenyl ring and pyrazole, chelate or thiazole rings (55–70°) were found for nickel complex **6a**. Hence, it is conceivable that this observation might be attributed to the coordination number. The higher number for nickel (6) than for copper (5) results in bigger steric hindrance forcing bigger twist of phenyl rings. Moreover, in the reported compounds the N1 chelate and sulfur rings form angles of at least 12.54°, which differ significantly from 0.77° found for **1a**. The adjacent rings, despite being fused, can form angles up to 14.71°. For complexes **6a** and **8a** the angles between the N1 pyrazole and S7 rings range from 14.0° to 17.7°. Hence, we observe some flexibility of this ligand, which adopts conformation dependent on the crystal network and possible interactions. For complexes **1b**, **6a** and **8a**, coordinated *via* N10 nitrogen from the aromatic ring, we observe smaller angles for the N1 pyrazole and chelate rings. For **5b** bearing only the pyrazole and chelate rings these angles are slightly bigger. Therefore, the lack of an additional phenyl ring and of the thiazole ring results in two important consequences: (i) the sulfur atom participates in the coordination of the metal ion, (ii) the lack of the thiazole ring allows for bigger conformational flexibility, as presented by a bigger value of the dihedral angle created between the N1 pyrazole and chelate rings. This is confirmed by the results obtained by Radosavljević *et al.*[34] for $Cd_2L''_2Cl_4$ (L″ = 3,5-dimethyl-1*H*-pyrazole-1-carbothioamide). They showed that the pyrazole and chelate rings remain coplanar with an angle of 19.8(5)° being significantly bigger than in our structures. Similarly, for $[Cu_2L''_2Cl_4]$, $[Cu_2L''_2Br_2]$ and $[Co_2L''_2Cl_4]$ complexes these values were 15°, 24° and 16.3°, respectively.[26] The mutual conformation of L′ or L″ ligands in complexes described by the 1 : 2 metal : pyrazole ligand stoichiometric ratio usually ranges from 50–60° in the reported structures. The values observed for the structures of $[ZnL^1_2(H_2O)]\cdot 2DMSO$ and $[ZnL^2_2(H_2O)]\cdot 2DMSO$ (L^1 and L^2 are 5-oxo-1*H*-pyrazole-1-carbothioamide derivatives) are 51.54° and 56.80°, being very similar to those observed for the reported structures.[35] Casas *et al.*[36] presented three complexes formulated as $[ZnL^4_2]\cdot 0.5H_2O[CdL^2_2(H_2O)]\cdot 2DMSO[CdL^5_2(DMSO)]\cdot DMSO$ with these angles being +78°, +55.9° and 22°, respectively. These data show that two ligands being pyrazole derivatives can adopt a mutual orientation in a very broad range. In our copper and nickel complexes, there are two pyrazole ligands in the coordination sphere and they are rather strongly twisted. Both fused systems in the reported compounds were found inclined at an angle 68.92° (**6a**), 52.20° (**8a**), 43.59° and 63.94° (**5b**) revealing a significant twist.

Biological assay

The cytotoxicity of the ligands (**a**, **b**) and their cobalt(II), nickel(II) and copper(II) complexes **1a–9a**, **1b–9b** was measured against human melanoma WM-115 cells as well as leukemia promyelocytic HL-60 and lymphoblastic NALM-6 cells. Cisplatin and carboplatin were used as the reference compounds.[37] Cells were exposed to a broad range of drug concentrations for 48 h and cell viability was analyzed by MTT assay. IC_{50} values of ligands and their complexes are shown in Table 2.

The ligand **a** was inactive in the case of WM-115 cells but expressed moderate cytotoxicity against NALM-6 and HL-60 leukemia cells. The ligand **b** was not toxic to the tested tumor cell lines. In both cases, the coordination of a metal to the ligand increased their cytotoxic activity.

The highest cytotoxic activity has been observed for cobalt(II) complexes **3a**, **1b**, **3b** and copper(II) complexes **8a**, **7b** against NALM-6 cells (IC_{50} coefficient in the range from 5.4 to 16.7 μM), and for copper(II) complexes **8a**, **7b**, **9b** against the melanoma WM-115 cell line (IC_{50} coefficient in the range from 4.9 to 20.6 μM). It should also be mentioned that significant cytotoxicity (IC_{50} coefficient in the range from 11.5 to 20.6 μM) among the metal complexes with 2-(3,5-dimethyl-1*H*-pyrazole-1-yl)-4-phenyl-1,3-thiazole (**a**) against the all cell lines was exhibited by ionic

Table 2 Cytotoxicity of the ligands and their metal(II) complexes **1a–9a**, **1b–9b** expressed as the IC_{50} values (in μM)

Compound	IC_{50}[a] [μM] HL-60	NALM-6	WM-115
a	82.6 ± 3.5	82.1 ± 1.6	945.0 ± 44.4
1a	48.4 ± 3.4	29.8 ± 5.5	289.1 ± 52.6
2a	55.9 ± 0.6	36.4 ± 1.8	277.5 ± 25.7
3a	46.6 ± 2.8	16.1 ± 1.1	78.1 ± 5.9
5a	64.3 ± 1.6	61.1 ± 1.4	434.3 ± 44.8
6a	47.1 ± 3.8	50.4 ± 1.4	251.3 ± 28.4
7a	37.9 ± 2.1	54.1 ± 2.9	64.7 ± 3.2
8a	11.5 ± 0.9	16.7 ± 0.5	20.6 ± 2.4
9a	45.4 ± 3.6	54.1 ± 4.4	60.7 ± 2.5
b	583.9 ± 84.3	569.3 ± 21.9	> 1000
1b	65.0 ± 3.1	9.1 ± 0.2	78.1 ± 15.2
3b	47.5 ± 1.67	8.9 ± 0.2	66.0 ± 3.5
4b	60.7 ± 1.45	63.1 ± 2.2	184.9 ± 22.8
5b	50.6 ± 3.8	51.6 ± 1.6	74.7 ± 6.8
6b	53.1 ± 0.9	52.7 ± 0.6	74.9 ± 3.9
7b	5.3 ± 0.2	5.4 ± 0.2	4.9 ± 0.2
8b	53.3 ± 3.0	50.3 ± 5.3	35.4 ± 4.2
9b	56.1 ± 7.2	56.7 ± 3.0	5.5 ± 0.6
Cisplatin[b]	0.8 ± 0.1	0.7 ± 0.3	18.2 ± 4.3
Carboplatin[b]	4.3 ± 1.3	0.7 ± 0.2	422.2 ± 50.2

[a] IC_{50} – concentration of a tested compound required to reduce the fraction of surviving cells to 50% of that observed in the control, non-treated cells. Mean values of IC_{50} (in μM) ± S.D. from 4 experiments are presented. [b] See the literature.[38]

copper(II) complex **8a**. Copper(II) complex **7b** (with 3,5-dimethyl-1*H*-pyrazole-1-carbothioamide) exhibited the highest cytotoxic activity against all the tested cell lines (IC_{50} coefficient in the range from 4.9 to 5.4 μM). This compound with an IC_{50} of 5.3 μM expressed similar activity against leukemia promyelocytic HL-60 cells and was almost four times more effective (IC_{50} = 4.9 μM) in the case of melanoma WM-115 cells when compared to cisplatin (IC_{50} 18.2 μM).

The presence of the carbothioamide moiety in the structure improved the activity of these metal complexes significantly, compared to the corresponding compounds with the 4-phenylthiazole-derived ligand in the case of melanoma WM-115 cells.

All the metal(II) complexes, besides copper complexes with the thiosemicarbazone-derived ligand (**7b–9b**), showed higher cytotoxic activity to both acute leukemia HL-60 and NALM-6 cell lines than against the melanoma cells, whereas these copper compounds, especially compound **9b**, exhibited selective cytotoxicity against melanoma WM-115 cells.

The lowest activity ($IC_{50} > 184$ μM) against WM-115 cells showed cobalt(II) and nickel(II) complexes **1a**, **2a**, **5a**, **4b**. However, the cytotoxicity of almost all the metal(II) complexes was higher than that of carboplatin against these tumor cells.

We also decided to examine the cytotoxicity of the more promising compounds (**1b**, **3b**, **7b**) against normal human umbilical vein endothelial cells (HUVECs). Analysis of the cytotoxicity data revealed that **1b** and **3b** presented higher effectiveness against NALM-6 leukemia cells compared to the normal HUVECs (IC_{50} = 73.0 μM and IC_{50} = 38.6 μM respectively). The cytotoxic activity of **7b** against healthy cells was also high with IC_{50} = 5.1 μM.

Conclusions

In this paper we have described the synthesis of novel cobalt(II), nickel(II) and copper(II) complexes with *N*,*N*-donor phenylthiazole and with an *N*,*S*-donor thiosemicarbazone-derived ligand. The structures of these complexes were confirmed by spectral and elemental analysis. The molecular structures of four complexes **1a**, **6a**, **8a** and **5b** were confirmed by X-ray analysis. We found that the M–N10 bonds are usually by 0.05–0.07 Å longer than the metal–pyrazole nitrogen bond, but for complex **8a** this elongation is much bigger (0.3 Å). In the reported structures two kinds of nitrate coordination were found: the monodentate in **8a** and bidentate in **5b**. We observed the influence of the coordination number and of substituents on the conformation of the complexes. In all analyzed complexes hydrogen bonds played a principal role in the crystal network formation. Having compared the coordination modes observed for both studied ligands we have concluded that aliphatic sulfur can participate in metal binding and sometimes even in bridge formation, whereas thiazole sulfur is not involved in the coordination. At least partially this effect can be ascribed to bigger conformational flexibility.

A cytotoxic study demonstrates that the coordination compounds of copper(II) with the both ligands were more effective against the skin melanoma WM-115 cells when compared to cobalt(II) and nickel(II) compounds. It should be noted that higher cytotoxic activity was observed in WM-115 cultures treated with copper(II) complexes containing the *N*,*S*-donor thiosemicarbazone ligand than in those treated with copper(II) complexes containing the *N*,*N*-donor phenylthiazole ligand. A Cu(II) complex of 3,5-dimethyl-1*H*-pyrazole-1-carbothioamide (**7b**) exhibits the highest cytotoxic activity towards all tested cell lines. Cytotoxic effectiveness of this complex and of another copper(II) complex with thiosemicarbazone-derived ligand (**9b**) against melanoma WM-115 cells was about four times higher than that of cisplatin. Unfortunately, **7b** complex also showed a high toxic effect to the noncancerogenic HUVECs.

Preliminary experiments also showed promising cytotoxic activity of copper(II) compound **8a**. Its activity was the greatest among the complexes with the 4-phenylthiazole derivative, which could be ascribed to its different ionic structure. Therefore, more experimental work is necessary to confirm the cytotoxic behavior and the mechanism of action of this copper(II) complex.

Experimental

Materials and methods

All substances were used without further purification. Metal(II) chloride, nitrate and perchlorate salts were purchased from Aldrich. DMSO-d_6 solvents for NMR spectroscopy were obtained from Dr Glaser AG Basel. Solvents for synthesis (acetonitrile, dichloromethane, diethyl ether, dimethylformamide, ethyl acetate, and methanol) were reagent grade or better and were dried according to standard protocols.[38] The melting points were determined using an Electrothermal 1A9100 apparatus and they are uncorrected. The ^1H NMR spectra were registered at 300 MHz on a Varian Mercury spectrometer. The IR spectra were recorded on KBr pellets on an FT-IR-8400S Shimadzu spectrophotometer. The FAB-MS data were determined on a Finnigan Matt 95 mass spectrometer (NBA, Cs^+ gun operating at 13 keV). For the new compounds elemental analyses (C, H and N) were performed using a Perkin Elmer PE 2400 CHNS analyzer.

Synthesis of the ligands

Synthesis of ligand 2-(3,5-dimethyl-1*H*-pyrazole-1-yl)-4-phenyl-1,3-thiazole (**a**) was based on the method described previously with some modifications.[39] Acetylacetone (480 mg, 4.8 mmol) and 2-hydrazino-4-phenylthiazole (920 mg, 4.8 mmol) were stirred in anhydrous methanol (7 ml) and catalytic amounts of *p*-toluenesulfonic acid were added to a stirred solution. The reaction was monitored by thin-layer chromatography (TLC) using a silica gel on aluminum sheets with fluorescent dye F254 and a 20/80 mixture of acetone/chloroform as the mobile phase. After 3 h of refluxing, the concentration of the solution to half of its initial volume gave a solid that was filtered out and dried under reduced pressure. Yield: 969 mg, 85.0%, mp 102.2–103.5 °C. FTIR (KBr cm^{-1}): 3083s, 1603m, 1573s, 1539s, 1479m, 1026m, 685m. ^1H NMR (DMSO-d_6) δ (ppm): 2.32 (s, 3H, C(3)–CH_3 pyrazole) 2.80 (s, 3H, C(5)–CH_3 pyrazole), 6.03 (s, 1H C(4) pyrazole), 7.27 (m, 1H, phenyl), 7.35 (m, 2H, phenyl), 7.77 (s, 1H, thiazole), 7.90 (m, 2H, phenyl).

The 3,5-dimethyl-1*H*-pyrazole-1-carbothioamide (**b**) was prepared as described elsewhere.[25] Hydrazinecarbothioamide (1.2 g, 13.2 mmol) was dissolved in HCl (80 ml, 0.05 M) and pentano-2,4-dione (1.3 ml, 13.2 mmol) was added dropwise to the stirred mixture. After stirring for 2 h and 3 h incubation at room temperature, a white precipitate was filtered off, washed with water and dried under reduced pressure. Yield: (1.52 g, 85.0%), mp 92.3–93.7 °C. FT-IR (KBr, cm^{-1}): 3241s, 3134s, 2976w, 1600s, 1576s, 1341m, 880s, 808m. ^1H NMR (700 MHz, DMSO-d_6) δ (ppm): 2.17 (d, 6H, C(3)–CH_3, C(5)–CH_3 pyrazole), 6.19 (s, 1H, C(4)pyrazole), 9.13 (s, 1H, NH_2), 9.54 (s, 1H, NH_2).

Synthesis of the complexes

Caution! Perchlorate salts are potentially explosive and were handled only in small quantities with care.

Cobalt(II) complex (1a). Cobalt(II) chloride hexahydrate $CoCl_2{\cdot}6H_2O$ (48.5 mg, 0.2 mmol) was dissolved in 1.0 ml of methanol and was added dropwise at room temperature to a stirred solution of ligand **a** (52.0 mg, 0.2 mmol) in ethyl acetate (5.0 ml). The reaction solution was stirred for 12 hours at room temperature. The resulting green crystals of **1a** were obtained by the diffusion of diethyl ether into the mixture. Yield: (57.8 mg, 69%), mp 296.5–298.5 °C. Anal. calcd for **1a** $C_{14}H_{13}N_3SCoCl_2{\cdot}2H_2O$ (421.15 g mol^{-1}) C, 39.93%; H, 4.07%; N, 9.98%; found: C, 40.09%; H, 4.22%; N, 10.10%. FTIR (KBr cm^{-1}): 3091w, 1623w, 1574m, 1502s, 1020w, 686m. MS-FAB (*m*/*z*): 256.1 (10%) $[\mathbf{a}]^+$, 313.1 (90%) $[(\mathbf{a})Co]^+$, 349.1 (100%) $[(\mathbf{a})CoCl]^+$.

Cobalt(II) complex (2a). Cobalt(II) nitrate hexahydrate $Co(NO_3)_2{\cdot}6H_2O$ (68.9 mg, 0.24 mmol) was dissolved in 1 ml of methanol and was added dropwise at room temperature to a stirred solution of ligand **a** (60.4 mg, 0.24 mmol) in ethyl acetate (5 ml). The reaction solution was stirred for 12 hours at room temperature. The resulting maroon solid **2a** was obtained by the diffusion of diethyl ether into the mixture. Yield: (35.0 mg, 25.5%), mp dec. >282.3 °C. Anal. calcd for **2a** $C_{14}H_{13}N_3SCoN_2O_6{\cdot}1.5C_4H_8O_2{\cdot}0.5H_2O$ (579.36 g mol^{-1}) C 41.24%; H, 4.52%; N, 12.09%. Found: C, 40.89%; H, 4.42%; N, 12.26%. FTIR (KBr cm^{-1}): 3367br, 3098m, 1736m, 1647w, 1576m, 1506s, 1379s, 1011w, 845m, 698m. MS-FAB (*m*/*z*): 256.0 (25%) $[\mathbf{a}]^+$, 313.1 (15%) $[(\mathbf{a})Co]^+$, 376.1 (100%) $[(\mathbf{a})CoNO_3]^+$.

Cobalt(II) complex (3a). Cobalt(II) perchlorate hexahydrate $Co(ClO_4)_2{\cdot}6H_2O$ (43.9 mg, 0.12 mmol) was added dropwise at room temperature to a stirred solution of ligand **a** (61.3 mg, 0.24 mmol) in ethyl acetate (8 ml). The reaction solution was stirred for 24 hours at room temperature. The resulting maroon solid **3a** was obtained by the diffusion of diethyl ether into the mixture. Yield: (81.2 mg, 84%), mp 299.8–302.3 °C. Anal. calcd for **3a** $C_{28}H_{26}N_6S_2CoCl_2O_8{\cdot}2H_2O$ (804.45 g mol^{-1}) C, 41.81%; H, 3.76%; N, 10.45%. Found: C, 41.89%; H, 3.23%; N, 10.33%. FTIR (KBr cm^{-1}): 3363br, 3100m, 1630m, 1578s, 1503s, 1116s, 1026s, 689m, 629m. MS-FAB (*m*/*z*): 256.2 (80%) $[\mathbf{a}]^+$, 313.1 (74%) $[(\mathbf{a})Co]^+$, 413.2 (96%) $[(\mathbf{a})CoClO_4]^+$, 569.3 (52%) $[(\mathbf{a})_2Co]^+$, 669.3 (100%) $[(\mathbf{a})_2CoClO_4]^+$.

Nickel(II) complex (5a). Nickel(II) nitrate hexahydrate $Ni(NO_3)_2{\cdot}6H_2O$ (74.5 mg, 0.26 mmol) was dissolved in 2 ml of methanol and was added dropwise at room temperature to a stirred solution of ligand **a** (65.4 mg, 0.26 mmol) in ethyl acetate (8 ml). The reaction solution was stirred for 24 hours at room temperature. A light green-blue crystalline product was obtained by the diffusion of diethyl ether into the mixture. Yield: (79.0 mg, 39%), mp 153.6–155.2 °C. Anal. calcd for **5a** $C_{14}H_{13}N_3SNiN_2O_6{\cdot}CH_3OH$ (470.03 g mol^{-1}) C, 38.33%; H, 3.65%; N, 14.90%. Found: C, 38.31%; H, 3.41%; N, 14.66%. FTIR (KBr cm^{-1}): 3353br, 3104m, 1580m, 1536w, 1511s, 1383s, 1022m, 825m, 687m. ^1H NMR (DMSO-d_6) δ (ppm): 2.15 (s, 3H, C(3)–CH_3 pyrazole); 2.67 (s, 3H, C(5)–CH_3 pyrazole); 6.17 (s, 1H, C(4) pyrazole); 7.30 (t, 1H, C(phenyl), $^3J_{HH}$ = 7.7 Hz), 7.40 (t, 2H, C(phenyl) $^3J_{HH}$ = 7.7 Hz), 7.80 (s, 1H, C thiazole); 7.90 (d, 2H, C(phenyl), $^3J_{HH}$ = 7.7 Hz). MS-FAB (*m*/*z*): 256.2 (5%) $[\mathbf{a}]^+$, 314.0 $[(\mathbf{a})Ni]^+$, 375.1 (100%) $[(\mathbf{a})NiNO_3]^+$.

Nickel(II) complex (6a). Nickel(II) perchlorate hexahydrate $Ni(ClO_4)_2{\cdot}6H_2O$ (44.5 mg, 0.12 mmol) was dissolved in 2 ml of methanol (1.0 ml) and was added dropwise at room temperature to a stirred solution of ligand **a** (62.2 mg, 0.24 mmol) in ethyl acetate (10 ml). A green-blue crystalline product was obtained by the diffusion of diethyl ether into the mixture. Yield: (68.6.0 mg, 70.0%), mp dec. >299.1 °C. Anal. calcd for **6a** $C_{28}H_{26}N_6S_2NiCl_2O_8{\cdot}2H_2O$ (804.19 g mol^{-1}) C, 41.82%; H, 3.76%; N, 10.45%. Found: C, 41.69%; H, 3.46%; N, 10.45%. FTIR (KBr cm^{-1}): 3390br, 3084m, 1654m, 1582s, 1538s, 1505s, 1031s, 700m, 1085s, 623m. ^1H NMR (DMSO-d_6) δ (ppm): 2.16 (s, 3H, C(3)–CH_3 pyrazole); 2.67 (s, 3H, C(5)–CH_3 pyrazole); 6.17 (s, 1H, C(4) pyrazole); 7.30 (t, 1H, C(phenyl), $^3J_{HH}$ = 7.0 Hz), 7.41 (t, 2H, C(phenyl), $^3J_{HH}$ = 7.0 Hz); 7.81 (s, 1H, C(thiazole)); 7.89 (d, 2H, C(phenyl), $^3J_{HH}$ = 7.0 Hz). MS-FAB (*m*/*z*): 256.0 (10%) $[\mathbf{a}]^+$, 313.1 (50%) $[(\mathbf{a})Ni]^+$, 412.1 (80%) $[(\mathbf{a})NiClO_4]^+$, 568.1 (25%) $[(\mathbf{a})_2Ni]^+$, 667.1 (100%) $[(\mathbf{a})_2NiClO_4]^+$.

Copper(II) complex (7a). Copper(II) chloride dihydrate $CuCl_2{\cdot}2H_2O$ (54.9 mg, 0.2 mmol) was dissolved in 1.0 ml of methanol and was added dropwise at room temperature to a stirred solution of ligand **a** (50.5 mg, 0.2 mmol) in ethyl acetate (10.0 ml). The stirring was continued for 24 hours at room temperature and the reaction mixture was left standing overnight. A yellow micro-crystalline product was obtained, filtered off and dried in vacuum. Yield: (73.0 mg, 71%), mp 163.9–166.0 °C. Anal. calcd for **7a** $C_{14}H_{13}N_3SCoCl_2{\cdot}4H_2O$ (461.79 g mol^{-1}) C, 36.41%; H, 4.58%; N, 9.10%; found: C, 36.80%; H, 4.98%; N, 9.69%. FTIR (KBr cm^{-1}): 3366br, 3091m, 1623m, 1574s, 1502s, 1020m, 686w. MS-FAB (*m*/*z*): 256.1 (35%) $[\mathbf{a}]^+$, 318.0 (100%) $[(\mathbf{a})Cu]^+$, 353.0 (75%) $[(\mathbf{a})CuCl]^+$.

Copper(II) complex (8a). Copper(II) nitrate trihydrate $Cu(NO_3)_2{\cdot}3H_2O$ (22.3 mg, 0.09 mmol) was dissolved in 0.5 ml of methanol and was added dropwise at room temperature to a stirred solution of ligand **a** (23.6 mg, 0.09 mmol) in ethyl acetate (5 ml). The reaction solution was stirred for 12 hours at room temperature. The resulting dark green solid **8a** was obtained by the diffusion of diethyl ether into the mixture. Yield: (35.0 mg, 72%), mp 155.2–156.6 °C. Anal. calcd for **8a** $C_{56}H_{52}N_{18}O_{18}S_4Cu_3$ (1583.80 g mol^{-1}) C 42.47%; H, 3.31%; N, 15.92%. Found: C, 42.35%; H, 3.41%; N, 15.46%. FTIR (KBr cm^{-1}): 3107w, 1635w, 1573s, 1506s, 1381s, 1009m, 829m, 699w. MS-FAB(+) (*m*/*z*): 318.2 (100%) $[(\mathbf{a})Cu]^+$, 573.3 (30%) $[(\mathbf{a})_2Cu]^+$, 637.3 (5%) $[(\mathbf{a})_2CuNO_3]^+$. MS-FAB(−) (*m*/*z*): 186.8 (100%) $[Cu(NO_3)_4]^{2-}$, 311.9 (10%) $[Cu(NO_3)_2]^-$.

Copper(II) complex (9a). Copper(II) perchlorate hexahydrate $Cu(ClO_4)_2{\cdot}6H_2O$ (40.2 mg, 0.11 mmol) was dissolved in 1.0 ml of methanol and was added dropwise at room temperature to a stirred solution of ligand **a** (56.1 mg, 0.22 mmol) in ethyl acetate (10 ml). The reaction solution was stirred for 24 hours at room temperature. The resulting maroon solid **9a** was obtained by the diffusion of diethyl ether into the mixture. Yield: (64.0 mg, 84%), mp 233.2–235.3 °C. Anal. calcd for **9a** $C_{28}H_{26}N_6S_2CuCl_2O_8{\cdot}0.5H_2O$ (782.02 g mol^{-1}) C, 43.01%; H, 3.48%; N, 10.75%. Found: C, 43.01%; H, 3.89%; N, 10.32%. FTIR (KBr cm^{-1}): 3395br, 3105m, 1574m, 1533w, 1507s, 1108m, 1015s, 701w, 623m. MS-FAB (*m*/*z*): 256.1 (35%) $[\mathbf{a}]^+$, 318.1 (100%) $[(\mathbf{a})Cu]^+$, 418.1 (5%) $[(\mathbf{a})CuClO_4]^+$, 574.3 (30%) $[(\mathbf{a})_2Cu]^+$.

Cobalt(II) complex (1b). Cobalt(II) chloride hexahydrate $CoCl_2{\cdot}6H_2O$ (95.5 mg, 0.4 mmol) was dissolved in 0.5 ml of methanol and was added dropwise at room temperature to a stirred solution of ligand **b** (62.3 mg, 0.4 mmol) in ethyl acetate (7.0 ml). The stirring was continued for half an hour at room temperature and the reaction mixture was left standing overnight. A blue micro-crystalline product was obtained, filtered off and dried in vacuum. Yield: (52.5 mg, 55%), mp 180.0–182.1 °C. Anal. calcd for **1b** $C_6H_9N_3SCoCl_2$ (285.0 g mol^{-1}) C, 25.29%; H, 3.19%; N, 14.75%; found: C, 25.48%; H, 2.84%; N, 14.38%. FTIR (KBr, cm^{-1}): 3264s, 3155m, 2991w, 1627s, 1591s, 1341s, 842s, 779m. MS-FAB (*m*/*z*): 249.0 (45%) $[Co(\mathbf{b})Cl]^+$, 404.1 (23%) $[Co(\mathbf{b})_2Cl]^+$.

Cobalt(II) complex (3b). Cobalt(II) perchlorate hexahydrate $Co(ClO_4)_2{\cdot}6H_2O$ (84.0 mg, 0.23 mmol) was added at room temperature to a stirred solution of ligand **b** (71.2 mg, 0.46 mmol) in ethyl acetate (7 ml). The reaction solution was stirred for 12 hours at room temperature and was left standing overnight. The resulting pink micro-crystalline product was filtered off and dried. Yield: (55.5 mg, 84%), mp dec. >130 °C. Anal. calcd for **3b** $C_{12}H_{18}N_6S_2CoCl_2O_8{\cdot}2H_2O$ (604.19 g mol^{-1}) C, 23.86%; H, 3.67%; N, 13.91%. Found: C, 23.94%; H, 3.59%; N, 13.66%. FTIR (KBr, cm^{-1}): 3418br, 3253s, 3142s, 2927w, 1634s, 1596s, 1343s, 1114s, 860s, 777s, 624m. MS-FAB (*m*/*z*): 213.0 (18%) $[(\mathbf{b})Co]^+$, 313.0 (55%) $[(\mathbf{b})CoClO_4]^+$, 368.0 (100%) $[(\mathbf{b})_2Co]^+$, 468.0 (18%) $[(\mathbf{b})_2CoClO_4^-]^+$.

Nickel(II) complex (4b). Nickel(II) chloride anh. $NiCl_2$ (49.58 mg, 0.38 mmol) was dissolved in 0.5 ml of methanol and was added dropwise at room temperature to a stirred solution of ligand **b** (59.1 mg, 0.38 mmol) in ethyl acetate (5.0 ml). The reaction solution was stirred for 12 hours at room temperature. The resulting orange-brown crystals of **4b** were obtained by the diffusion of diethyl ether into the mixture. Yield: (74.5 mg, 69%), mp 145.8–146.75 °C. Anal. calcd for **4b** $C_6H_9N_3SNiCl_2$ (284.88 g mol^{-1}) C, 25.31%; H, 3.19%; N, 14.75%; found: C, 25.29%; H, 2.93%; N, 14.25%. FTIR (KBr, cm^{-1}): 3364s, 3254s, 3074m, 2995w, 1626s, 1616s, 1588s, 1339s, 863s, 779m. ^1H NMR (DMSO-d_6) δ (ppm): 1.90 (s, 3H, C(3)–CH_3 pyrazole), 2.40, (s, 3H, C(5)–CH_3 pyrazole); 5.92 (s, 1H, C(4) pyrazole); 8.86 (s, 1H, NH_2); 9.27 (s, 1H, NH_2). MS-FAB (*m*/*z*): 213.0 (40%) $[(\mathbf{b})Ni]^+$, 249.0 (100%) $[(\mathbf{b})NiCl]^+$.

Nickel(II) complex (5b). Nickel(II) nitrate hexahydrate $Ni(NO_3)_2{\cdot}6H_2O$ (104.7 mg, 0.36 mmol) was dissolved in 2 ml of methanol and was added dropwise at room temperature to a stirred solution of ligand **b** (54.5 mg, 0.36 mmol) in ethyl acetate (6 ml). The reaction solution was stirred for 12 hours at room temperature. A dark green crystalline product was obtained by the diffusion of diethyl ether into the mixture. Yield: (69.8 mg, 26%), mp dec. >171.6 °C. Anal. calcd for **5b** $C_{12}H_{18}N_6S_2NiN_2O_6{\cdot}0.5H_2O$ (502.29 g mol^{-1}) C, 28.69%; H, 3.81%; N, 22.31%. Found: C, 28.66%; H, 3.24%; N, 21.84%. FTIR (KBr, cm^{-1}): 3286br, 3249s, 3114s, 2976w, 1641s, 1586s, 1383s, 1348s, 863s, 834m, 783m. ^1H NMR (DMSO-d_6) δ (ppm): 2.14 (s, 3H, C(3)–CH_3 pyrazole); 2.63 (s, 3H, C(5)–CH_3 pyrazole); 6.16 (s, 1H, C(4) pyrazole); 9.11 (s, 1H, NH_2); 9.52 (s, 1H, NH_2). MS-FAB (*m*/*z*): 213.0 (20%) $[(\mathbf{b})Ni]^+$, 275.0 (100%) $[(\mathbf{b})NiNO_3]^+$, 368.0 (64%) $[(\mathbf{b})_2Ni]^+$, 430.2 (48%) $[(\mathbf{b})NiNO_3]^+$.

Nickel(II) complex (6b). Nickel(II) perchlorate hexahydrate $Ni(ClO_4)_2{\cdot}6H_2O$ (49.5 mg, 0.135 mmol) was dissolved in 1.0 ml of methanol (1.0 ml) and was added dropwise at room temperature to a stirred solution of ligand **b** (42.2 mg, 0.27 mmol) in ethyl acetate (4.0 ml). A green crystalline product was obtained by the diffusion of diethyl ether into the mixture. Yield: (35.0 mg, 53.4%), mp dec. >168.1 °C. Anal. calcd for **6b** $C_{18}H_{27}N_9S_3NiCl_2O_8$ (723.44 g mol^{-1}) C, 29.87%; H, 3.33%; N, 17.25%. Found: C, 29.80%; H, 3.76%; N, 17.40%. FTIR (KBr, cm^{-1}): 3202s, 3119s, 2984w, 1627s, 1589s, 1355s, 1103s, 875s, 776m, 623m. ^1H NMR (DMSO-d_6) δ (ppm): 2.14 (s, 3H, C(3)–CH_3 pyrazole); 2.62 (s, 3H, C(5)–CH_3 pyrazole); 6.16 (s, 1H, C(4) pyrazole); 9.10 (s, 1H, NH_2); 9.51 (s, 1H, NH_2). MS-FAB (*m*/*z*): 213.0 (3%) $[(\mathbf{b})Ni]^+$, 367.0 (100%) $[(\mathbf{b})_2Ni]^+$, 467.0 (20%) $[(\mathbf{b})_2NiClO_4]^+$.

Copper(II) complex (7b). This complex was synthesized according to the literature with some modifications.[26] Copper(II) chloride dihydrate $CuCl_2{\cdot}2H_2O$ (85.2 mg, 0.5 mmol) was dissolved in a mixture of ethyl acetate (4.0 ml) and methanol (0.5 ml) and was added dropwise at room temperature to a stirred solution of ligand **b** (77.6 mg, 0.5 mmol) in ethyl acetate (5.0 ml). The reaction solution was stirred for 24 hours at room temperature. The resulting gray-green solid product of **7b** was obtained by the diffusion of diethyl ether into the mixture. Yield: (128.00 mg, 88%), mp 164.8–166.2 °C. Anal. calcd for **7b** $C_6H_9N_3SCuCl_2$ (289.68 g mol^{-1}) C, 24.88%; H, 3.13%; N, 14.51%; found: C, 24.72%; H, 3.14%; N, 14.48%. FTIR (KBr cm^{-1}): 3296s, 3106m, 1621s, 1588m, 1346s, 999m, 847m. Other details of the synthesis, and characterization of this complex were described in our previous article.[25]

Copper(II) complex (8b). Copper(II) nitrate trihydrate $Cu(NO_3)_2{\cdot}3H_2O$ (56.9 mg, 0.24 mmol) was dissolved in 2 ml of methanol and was added dropwise at room temperature to a stirred solution of ligand **b** (73.0 mg, 0.48 mmol) in ethyl acetate (12 ml). The stirring was continued for 2 hours at room temperature and the reaction mixture was left standing overnight. A brown-yellow micro-crystalline product was obtained, filtered off and dried in vacuum. Yield: (70.5 mg, 60%), mp 135.2–136.6 °C. Anal. calcd for **8b** $C_{12}H_{18}N_6S_2CuN_2O_6{\cdot}C_4H_8O_2{\cdot}3.5H_2O$ (649.04 g mol^{-1}) C, 29.61%; H, 5.12%; N, 17.26%. Found: C, 29.74%; H, 5.66%; N, 17.16%. FTIR (KBr, cm^{-1}): 3462br, 3284s, 3146m, 3109w, 2983w, 1734m, 1573s, 1383s, 1350s, 810m, 750m. MS-FAB (*m*/*z*): 218.0 (20%) $[(\mathbf{b})Cu]^+$, 281.1 (100%) $[(\mathbf{b})CuNO_3]^+$, 437.2 (48%) $[(\mathbf{b})CuNO_3]^+$.

Copper(II) complex (9b). Copper(II) perchlorate hexahydrate $Cu(ClO_4)_2{\cdot}6H_2O$ (60.9 mg, 0.22 mmol) was dissolved in 1.0 ml of methanol and was added dropwise at room temperature to a stirred solution of ligand **b** (68.0 mg, 0.44 mmol) in ethyl acetate (7.0 ml). The stirring was continued for half hour at room temperature and the reaction mixture was left standing overnight. A brown-green micro-crystalline product was obtained, filtered off and dried in vacuum. Yield: (51.7 mg, 43%), mp 159.9–160.5 °C. Anal. calcd for **9b** $C_{18}H_{27}N_9S_3CuCl_2O_8{\cdot}C_4H_8O_2{\cdot}3H_2O$ (870.09 g mol^{-1}) C, 30.37%; H, 4.75%; N, 14.49%. Found: C, 30.05%; H, 4.29%; N, 14.57%. FTIR (KBr, cm^{-1}): 3524br, 3288s, 3149m, 3113m, 2983w, 1716m, 1620m, 1574s, 1348s, 1120s, 812s, 750m, 623m. MS-FAB (*m*/*z*): 219.0 (3%) $[(\mathbf{b})Cu]^{2+}$, 473.1 (20%) $[(\mathbf{b})_2CuClO_4]^+$.

Cells and cytotoxicity assay

Cell cultures. Human skin melanoma WM-115 cells as well as human leukemia promyelocytic HL-60 and lymphoblastic NALM-6 cell lines were used. Leukemia cells were cultured in RPMI 1640 medium supplemented with 10% fetal bovine serum and antibiotic (gentamicin, at 37 °C under a 5% CO_2/95% air atmosphere). For melanoma WM-115 cells Dulbecco's minimal essential medium (DMEM) instead of RPMI 1640 was used. In some cases normal human umbilical vein endothelial cells (HUVECs) were also used. HUVECs and all reagents for cell culture were purchased from Cascade Biologics (Portland, Oregon, USA). The HUVECs were cultured according to the manufacturer's instructions and the cells underwent 3e8 passages. Cells were grown at 37 °C in a humidified atmosphere of 5% CO_2 in air.

Cytotoxicity assay by MTT. The cytotoxicity of ligands, their complexes, carboplatin and cisplatin was determined by the MTT [3-(4,5-dimethylthiazol-2-yl)-2,5-diphenyltetrazolium bromide, Sigma, St. Louis, MO] assay as described.[37] Briefly, after 46 h of incubation with drugs, the cells were treated with the MTT reagent and incubation was continued for 2 h. MTT – formazan crystals were dissolved in 20% SDS and 50% DMF at pH 4.7 and absorbance was read at 562 and 630 nm on an ELISA – plate reader (ELX 800, Bio-Tek, USA). The values of IC_{50} (the concentration of the test compound required to reduce the cells survival fraction to 50% of the control) were calculated from concentration-response curves and used as a measure of cellular sensitivity to a given treatment. Stock solutions of ligands, metal complexes, carboplatin and cisplatin were freshly prepared in DMSO and diluted with complete culture medium to obtain a concentration range from 10^{-7}–10^{-3} M for ligands **a**, **b** and from 10^{-7}–5×10^{-4} M for metal complexes. DMSO concentration never exceeded 0.2% and had no influence on cell growth. As control, cultured cells were grown in the absence of drugs.

X-ray measurements. Diffraction data of all complexes were collected on Oxford Sapphire using a CCD area detector.[40] All structures were solved by direct methods and refined by full-matrix least-squares techniques on F^2 with SHELXL program.[41,42] The numerical absorption correction was applied for all crystals (RED171 package of programs, Oxford Diffraction, 2000[5]).

Heavy atoms were refined with anisotropic thermal displacement parameters. Positions of hydrogen atoms attached to carbon atoms were assigned at calculated positions, whereas positions of hydrogen atoms attached to oxygen or nitrogen atoms were found from electron density synthesis. All hydrogen atoms were refined with isotropic thermal displacement parameters fixed to a value of 20% or 50% higher than those of the corresponding C, N or O atoms. For compound **5b** several geometrical restraints (DFIX) were used for O73 and O83 diethyl ether molecules. In the final model of this compound there is a lack of hydrogen atoms attached to the O51 water molecule. Additionally, twining (twofold axis) was detected for this structure using ROTAX[43] program and the refinement process was carried out using TWIN and BASF commands. In complex **8a** the extinction coefficient was refined revealing a value of 0.0008. All figures were prepared in DIAMOND[44] and ORTEP-3.[45] The results of data collections and refinement have been summarized in Table 1.

CCDC 988739 (**1a**), 988743 (**6a**), 989127 (**8a**), and 988741 (**5b**).

Acknowledgements

Financial support from Collegium Medicum in Bydgoszcz, Department of Inorganic and Analytical Chemistry, grant No 411, the Medical University of Łódź, grant No. 503/3-066-02/503-01 (to E. Budzisz) and grant no 503/3-015-02/503-01 (to M. Rozalski) is gratefully acknowledged.

References

1 M. B. Ferrari, F. Bisceglie, G. G. Fava, G. Pelosi, P. Tarasconi, R. Albertini and S. Pinelli, *J. Inorg. Biochem.*, 2002, **89**, 36–44.
2 J. J. Alam, *Trends Biotechnol.*, 2003, **21**, 479–483.
3 K. Singh, M. S. Barwa and P. Tyagi, *Eur. J. Med. Chem.*, 2007, **42**, 394–402.

4 F. Basuli, S. M. Peng and S. Bhattacharya, *Inorg. Chem.*, 2000, **39**, 1120–1127.
5 D. C. Quenelle, K. A. Keith and E. R. Kern, *Antiviral Res.*, 2006, **71**, 24–30.
6 S. S. Karki, S. Thota, S. Y. Darj, J. Balzarini and E. De Clerc, *Bioorg. Med. Chem.*, 2007, **15**, 6632–6641.
7 Z. Afrasiabi, E. Sinn, S. Padhye, S. Dutta, S. Padhye, Ch. Newton, Ch. E. Anson and A. K. Powell, *J. Inorg. Biochem.*, 2003, **95**, 306–314.
8 B.-d. Wang, Z.-Y. Yang, M.-h. Lü, J. Hai, Q. Wang and Z.-N. Chen, *J. Organomet. Chem.*, 2009, **694**, 4069–4075.
9 Z. Afrasiabi, E. Sinn and J. Chen, *Inorg. Chim. Acta*, 2004, **357**, 271–278.
10 N. K. Singh, A. Srivastava, A. Sodhi and P. Ranjan, *Transition Met. Chem.*, 2000, **25**, 133–140.
11 J. García-Tojal, J. L. Pizarro, A. García-Orad, A. R. Pérez-Sanz, M. Ugalde, A. A. Díaz, J. L. Serra, M. I. Arriortua and T. Rojo, *J. Inorg. Biochem.*, 2001, **86**, 627–633.
12 Y. Subba Rao, B. Prathima, O. Hariprasad, N. Nagabhusan Reddy, M. Jagadeesh and A. Varada Reddy, *J. Chem. Pharm. Res.*, 2010, **2**, 292–299.
13 E. M. Jouad, G. Larcher and M. Allain, *J. Inorg. Biochem.*, 2001, **86**, 565–571.
14 N. K. Singh and S. B. Singh, *Indian J. Chem.*, 2001, **40**, 1070–1075.
15 M. Abid, S. M. Agarwal and A. Azam, *Eur. J. Med. Chem.*, 2008, **43**, 2035–2039.
16 S. Sharma, F. Athar, M. R. Maurya, F. Naqvi and A. Azam, *Eur. J. Med. Chem.*, 2005, **40**, 557–562.
17 N. Bharti, F. Athar, M. R. Maurya and A. Azam, *Bioorg. Med. Chem.*, 2004, **12**, 4679–4684.
18 J. Quiroga, P. Hernandez, B. R. Insuassty, R. Abonia, J. Cobo, A. Sanchez, M. Nogueras and J. N. Low, *J. Chem. Soc., Perkin Trans. 1*, 2002, 555–559.
19 I. Hutchinson, S. A. Jennings, B. R. Vishnuvajjala, A. D. Westwell and M. F. Stevens, *J. Med. Chem.*, 2002, **45**, 744–747.
20 S. Priya, J. Senthil Kumaran, N. Jayachandramani and S. Mahalakshmi, *Am. J. PharmTech Res.*, 2013, **3**, 607–616.
21 H. T. Fahmy and A. A. Bekhit, *Pharmazie*, 2002, **57**, 800–803.
22 Y. Y. Lu, C. M. Li, Z. Wang, C. R. Ross, J. Chen, J. T. Dalton, W. Li and D. D. Miller, *J. Med. Chem.*, 2009, **52**, 1701–1711.
23 M. M. Abd-Elzahera, S. A. Moustafa, A. A. Labib, H. A. Mousa, M. M. Ali and A. E. Mahmoud, *Appl. Organomet. Chem.*, 2012, **26**, 230–236.
24 C. Santini, M. Pellei, V. Gandin, M. Porchia, F. Tisato and C. Marzano, *Chem. Rev.*, 2014, **114**, 815–862.
25 M. Grazul, E. Besic-Gyenge, C. Maake, M. Ciolkowski, M. Czyz, R. K. O. Sigel and E. Budzisz, *J. Inorg. Biochem.*, 2014, **135**, 68–76.
26 I. Radosavljević Evans, J. A. K. Howard, L. E. M. Howard, J. S. O. Evans, Z. K. Jaćimović, V. S. Jevtović and V. M. Leovac, *Inorg. Chim. Acta*, 2004, **357**, 4528–4536.
27 K. Mészáros Szécsényi, V. M. Leovac, Z. K. Jaćimović and G. Pokol, *J. Therm. Anal. Calorim.*, 2003, **74**, 943–952.
28 K. Mészáros Szécsényi, V. M. Leovac, V. I. Češljević, A. Kovács, G. Pokol, G. Argay, A. Kálmán, G. A. Bogdanović, Z. K. Jaćimović and A. Spasojević-de Biré, *Inorg. Chim. Acta*, 2003, **353**, 253–262.
29 A. W. Addison, T. N. Rao, J. Reedijk, J. van Rijn and G. C. Verschoor, *J. Chem. Soc., Dalton Trans.*, 1984, 1349–1356.
30 G. A. Bogdanović, Z. K. Jaćimović and V. M. Leovac, *Acta Crystallogr., Sect. C: Cryst. Struct. Commun.*, 2005, **61**, m376–m379.
31 Z. K. Jaćimović, Z. D. Tomić, G. A. Bogdanović, E. Z. Ivegeš and V. M. Leovac, *Acta Crystallogr., Sect. C: Cryst. Struct. Commun.*, 1999, **55**, 1769–1771.
32 C. A. Bolos, P. V. Fanourgakis, P. C. Christidis and G. St. Nikolov, *Polyhedron*, 1999, **18**, 1661–1668.
33 I. Radosavljević Evans, J. A. K. Howard, K. Mészáros Szécsényi, V. M. Leovac and Z. K. Jacimović, *J. Coord. Chem.*, 2004, **57**, 469–476.
34 I. Radosavljević Evans, K. Mészáros Szécsényi and V. M. Leovac, *Acta Crystallogr., Sect. E: Struct. Rep. Online*, 2005, **61**, m641–m643.
35 J. S. Casas, M. V. Castaño, E. E. Castellano, J. Ellena, M. S. García-Tasende, A. Gato, A. Sánchez, L. M. Sanjuán and J. Sordo, *Inorg. Chem.*, 2002, **41**, 1550–1557.
36 J. S. Casas, M. V. Castaño, M. S. García-Tasende, E. Rodríguez-Castellón, A. Sánchez, L. M. Sanjuán and J. Sordo, *Dalton Trans.*, 2004, 2019–2026.
37 E. Budzisz, U. Krajewska and M. Rozalski, *Pol. J. Pharmacol.*, 2004, **56**, 473–478.
38 J. T. Wrobel, *Preparatyka i elementy syntezy organicznej*, PWN, Warsaw, Poland, 1983, pp. 9–52.
39 A. P. Novikova, I. Ya. Postovskii, S. M. Puchkova, L. A. Chechulina and T. N. Tuzhilkova, *Pharm. Chem. J.*, 1980, **14**, 383–386.
40 K. Brandenburg, *DIAMOND, Release 2.1e*, Crystal Impact GbR, Bonn, Germany, 2001.
41 *CrysAlis RED and CrysAlis CCD*, Oxford Diffraction Ltd, Abingdon, Oxfordshire, England, 2000.
42 L. J. Farrugia, *J. Appl. Crystallogr.*, 1997, **30**, 565–566.
43 R. I. Cooper, R. O. Gould, S. Parsons and D. J. Watkin, *J. Appl. Crystallogr.*, 2002, **35**, 168–174.
44 G. M. Sheldrick, *SHELXS97, SHELXL97 and CIFTAB*, University of Göttingen, Germany, 1997.
45 G. M. Sheldrick, *Acta Crystallogr., Sect. A: Found. Crystallogr.*, 2008, **A64**, 112–122.